Bone Response to Osteopontin-Functionalized Carboxyethylphosphonic Acid-Modified Implants. Experimental Study in a Minipig Model

Javier Aragoneses [1†], Nansi López-Valverde [1†], Antonio López-Valverde [2*], Cinthia Rodríguez [3], Bruno Macedo De Sousa [4] and Juan Manuel Aragoneses [5]

[1]Department of Medicine and Medical Specialties, Faculty of Health Sciences, Universidad Alcalá de Henares, Madrid, Spain, [2]Department of Surgery, Instituto de Investigación Biomédica de Salamanca (IB-SAL), University of Salamanca, Salamanca, Spain, [3]Department of Dentistry, Universidad Federico Henríquez y Carvajal, Santo Domingo, Dominican Republic, [4]Institute for Occlusion and Orofacial Pain Faculty of Medicine, Polo I-Edifício Cen-tral Rua Larga, University of Coimbra, Coimbra, Portugal, [5]Faculty of Dentistry, Universidad Alfonso X El Sabio, Madrid, Spain

Currently, dental implants have become a common and reliable treatment for restoring masticatory function in edentulous patients. Their surface topography is of great importance for the adhesion and remodeling of bone cells, both in the initial phases and over time, and different strategies have been proposed to improve the biological performance of conventional sandblasted, large-grit, acid-etched implant surfaces. Corrosion has been identified as one of the causes of implant failure due to contact with oral fluids. Carboxyethylphosphonic acid is a potent anticorrosive that would form stable bonds with titanium oxide, generating an organic layer on which modifications could be made to improve cell adhesion. Osteopontin is considered a molecule capable of improving the osseointegration of titanium. Our study evaluated the osseointegration capacity of titanium implants modified with carboxyethylphosphonic acid and functionalized with osteopontin in a minipig model. A total of 16 implants were inserted in the tibial diaphysis of two minipigs, 8 implants modified with carboxyethylphosphonic acid and functionalized with osteopontin from the experimental group and 8 from the control group with sandblasted, large-grit, acid-etched surface treatment. After 4 weeks, the animals were sacrificed and the samples were analyzed by histomorphometric analysis, assessing bone-implant contact, cortical bone-implant contact, percentage of new bone, peri-implant bone density and interthread bone area interthread. Statistical analysis was performed using SPSS v.18. Statistical significance was found between groups for the percentage of new bone ($p = 0.04$) and for interthread bone area interthread ($p = 0.01$). Functionalization of titanium surfaces by osteopontin may be of interest for conditioning bone remodeling in the early stages of osseointegration, although more *in vivo* studies are needed to determine its real influence in this aspect.

Keywords: titanium dental implants, carboxyethylphosphonic acid, osteopontin, surface bioactivation, mini-pig model

INTRODUCTION

Dental implants represent, nowadays, a reliable treatment for the rehabilitation of masticatory and esthetic function in totally or partially edentulous patients.

There are currently more than 1,300 different implant systems in terms of dimensions, design, thread, implant-abutment connections, surface topography and chemistry, wettability and surface modification (Junker et al., 2009). Surface topography, wettability and coatings contribute to the biological processes during osseointegration, as they are in close relationship with host osteoblasts during the osseointegration process (Smeets et al., 2016).

Despite the high long-term survival rate of dental implants, there is a low failure rate (1%), due to insufficient osseointegration during the first months of implant placement, although this rate is increased (5%) throughout implant survival, due to peri-implantitis (Chrcanovic et al., 2014; Smeets et al., 2014).

During implant osseointegration, in the contact osteogenesis phase, osteoblasts migrate towards the implant surface, differentiating and leading to the formation of new bone (Junker et al., 2009; Yuan et al., 2018).

The surface topography of dental implants is of great importance for adhesion, differentiation and bone remodeling, both during the initial phase of osseointegration and in the long term (Pellegrini et al., 2018). It is now considered that implant topography together with adequate implant bed preparation are the fundamental basis for clinical success (Le Guéhennec et al., 2007; Coelho et al., 2015; Ogle, 2015; Ren et al., 2021). Titanium (Ti) implants with a Sandblasted, Large-grit, Acid-etched (SLA) surface show superior bone-to-implant contact (50–60%) compared to other surface modifications, and the suitability of this type of surface in terms of overall osteogenic performance has been demonstrated *in vivo* (Mendonça et al., 2008; Zhang et al., 2020); however, there are techniques aimed at depositing hydroxyapatite and fluorapatite on the surface of Ti, which use a coating and blasting method at room temperature (CoBlast) that have reported excellent *in vitro* results (Dunne et al., 2015). In order to improve the biological performance of implant surfaces, biochemical and/or biophysical signals can be introduced by mechanical, physical or chemical methods (Mendonça et al., 2008; Dunne et al., 2015). Current research considers that the most representative hierarchical Ti surface is the SLA surface, which consists of micrometer-scale (20–40 µm) concavities produced by large-grain sandblasting and smaller submicrometer-scale (0.5–3 µm) concavities produced by acid etching. This type of surface has been shown to promote osseointegration and achieve satisfactory clinical results (Zhao et al., 2007).

Saliva contact corrosion has been pointed out as one of the failure mechanisms in dental implants (Corne et al., 2019), despite the fact that Titanium-Aluminum-Vanadium (Ti-6Al4V) alloys, nowadays employed in dental implantology, present additional advantages in terms of corrosion resistance, such as rupture potential, corrosion rate, pitting degradation and crevice corrosion (Klekotka et al., 2020). Carboxyethylphosphonic acid, $(HO2C-CR1H-CR2H-PO3H2)$ (CEPA), is characterized as a potent corrosion inhibitor. CEPA molecules can form stable bonds with passivated metal oxides, such as aluminum oxide (Al_2O_3) or Ti oxide (TiO_2),

producing an organic monolayer on which modifications could be made to improve cell adhesion and biocompatibility of dental implant surfaces (Aresti et al., 2021).

Surface bioactivation, on the other hand, is a biochemical method of surface modification based on the immobilization of proteins, enzymes or peptides that induce a specific cellular response at the bone-implant interface. Coating implant surfaces with bioactive molecules can modulate the biological response (Meng et al., 2016).

It has been shown that certain adhesion molecules, such as fibronectin, hyaluronic acid and osteopontin (OPN), are able to enhance osseointegration of Ti surfaces *in vitro*; moreover, OPN, from the extracellular matrix, would play an important role as a mediator in bone cell adhesion and bone mineralization (Icer and Gezmen-Karadag, 2018).

Therefore, the purpose of this research was to evaluate whether the application of OPN on CEPA-modified Ti implants would improve the osseointegration of dental implants by histomorphometric study of five parameters: bone-to-implant contact (BIC), cortical bone-to-implant contact (BICc), bone volume/total volume BV/TV, bone density inside the implant threads (BDIT) and perimplant bone density PBD, in comparison with implants with conventional surface treatment (SLA-type).

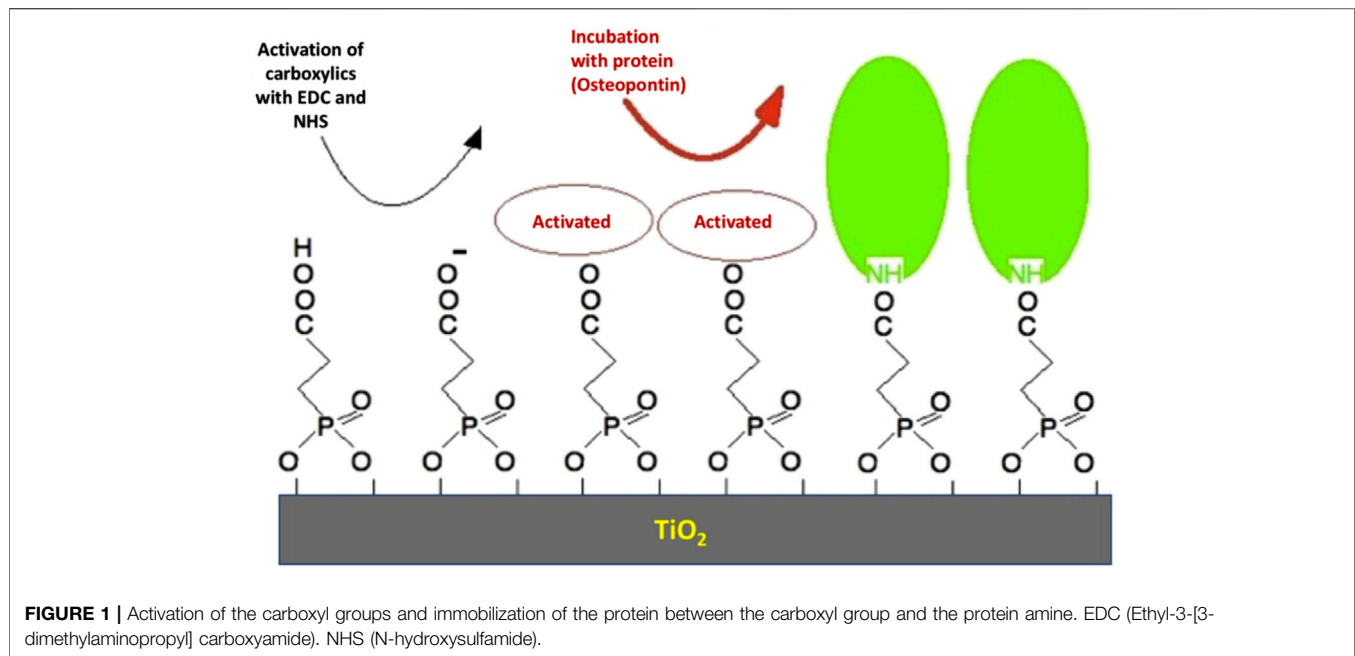# MATERIAL AND METHODS

Animal Model

The research was carried out on 2 Landrace (large white) minipigs, 18–2 weeks old at the beginning of the research and weighing between 20 and 25 kg (Distrizoo Animals SL, Madrid, Spain) and was approved by the Ethical Committee for Animal Experimentation of the Hospital Universitario Puerta de Hierro Majadahonda, Madrid, Spain, on 31 January 2013, Code CEEA: 017/2013.

Groups

Two groups were created: experimental group (G1) of implants modified with carboxyethylphosphonic acid and functionalized with OPN and control group (G2), with SLA surface treatment. A total of 16 implants were inserted (8 implants for each group). All G1 implants were inserted in the left tibiae and all G2 implants were inserted in the right tibiae. The randomization was carried out so that the operator was unaware of the difference between the experimental and control groups and thus did not affect their placement.

Implants and Surface Treatment

Self-tapping conical implants of Ti alloy grade 5 (Titanium 90%, Aluminum 6% and Vanadium 4%) of 4 mm in diameter and 10 mm in length, with internal conical connection (Galimplant®, Sarria, Lugo, Galicia, Spain) were used. The surface treatment using carboxyethylphosphonic acid was described in a previous investigation (Aragoneses et al., 2021). The OPN incubation procedure, at a dose of 0.06 µg per implant (Osteopontin human recombinant, expressed in HEX 293 Cells. Sigma-Aldrich Laboratory), was performed once the necessary carboxyl groups had been activated so that they were able to

FIGURE 1 | Activation of the carboxyl groups and immobilization of the protein between the carboxyl group and the protein amine. EDC (Ethyl-3-[3-dimethylaminopropyl] carboxyamide). NHS (N-hydroxysulfamide).

react with the amino groups of the protein (**Figure 1**). Sterilization was performed by gamma radiation at a dose of 25 KGy. The implants were sealed under the manufacturer's quality guarantee (Galimplant®, Sarria, Lugo, Galicia, Spain). The entire handling process was performed in a sterile environment and field. This sterilization method was preferred for the experimental group to avoid sterilization biases with the control group. Other methods, such as ethylene oxide, in addition to leaving residues detrimental to health, could damage the molecular structure of the coating and its susceptibility to degradation, although the effects of sterilization on the stability of the molecular structure and the mechanical properties of the coating itself are unclear. Some *in vitro* studies have shown that the early stages of mineralization are essentially independent of the sterilization method (Ueno et al., 2012; Türker et al., 2014).

Surgery

The surgical procedure was performed on the same day and by a single oral surgeon. During the 18 h prior to surgery, the animals were fasted from solid food, with free access to water consumption until 6 h before the start of surgery, to ensure the smallest possible volume of gastric contents and to avoid possible complications during the procedure, such as regurgitation of gastric contents. Premedication was performed intramuscularly in the lateral part of the neck (at the level of the trapezius and cleido-occipital muscles), using a combination of medetomidine at a dose of 0.01 mg/kg and ketamine (Ketolar®, Pfizer SL, Madrid, Spain) at a dose of 5 mg/kg, plus midazolam (Dormicum®, Roche SA., Basel, Switzerland) at a dose of 0.2 mg/kg and atropine (atropine Braun® BRAUN MEDICAL, SA Jaen, Spain) at a dose of 0.02 mg/kg. For anesthetic induction and endotracheal intubation, propofol (Diprivan®, AstraZeneca, Cambridge,United Kingdom) was administered intravenously. Once endotracheal intubation was

performed, an adequate anesthetic plane was maintained with propofol at a dose of 0.2–0.4 mg/kg/min. During the entire surgical procedure, the animal was monitored by means of electrocardiogram evaluation, capnography and temperature control; in addition, mechanical ventilation was established. Subsequently, epidural anesthesia was performed with bupivacaine (Bupivacaina®, Braun Medical, SA, Barcelona, Spain) and fentanyl (Fentanest®, Barcelona, Spain); in addition, local anesthesia was used infiltrated in the dermis where the incision would be made to access the tibia, in order to control hemorrhage through the vasoconstrictor of the anesthetic, in addition to enhance anesthesia and prevent animal suffering (Articaine 4% and adrenaline 1:100.000, Ultracain®, Normon, Madrid, Spain).

The location chosen in the tibia to insert the implants was the medial aspect of the diaphysis, away from the path of large blood vessels. The site chosen was away from the joints and muscle insertions. This ensured proper mobility and health of the animals from the time of surgery until the date of euthanasia. An Implantmed W&H® implant motor and a 20:1 contra-angle reducer (W&HWI-75E/KM) were used, with the surgical specifications indicated by the surgical sequence protocol for performing the osteotomy. The drilling of the bone beds was cooled with cold physiological serum (Vitulia Sol® Physiological Serum. 0.9%, ERN SA, Barcelona, Spain). Once the 4 osteotomies were performed in the tibia of the pig's leg, 4 implants (10 mm length x 4 mm Ø) were placed in each of the chosen tibias of the animal. Prior to implant insertion, a 4.1 mm Ø thread former was used on the bone cortex to prevent the insertion force from acting negatively on the coating. The implants in the left tibiae were from the experimental group (G1) and those in the right tibiae from the control group (G2). The suture was made by planes, the deepest one, using fast resorbable polyglactin of 5/0 thickness (VICRYL®, Johnson and Johnson SA, Madrid, Spain) and dermis and epidermis using non-resorbable braided silk of 3/0 thickness (Laboratorios Aragó, Barcelona, Spain) (**Figure 2**). After surgery, each animal was given
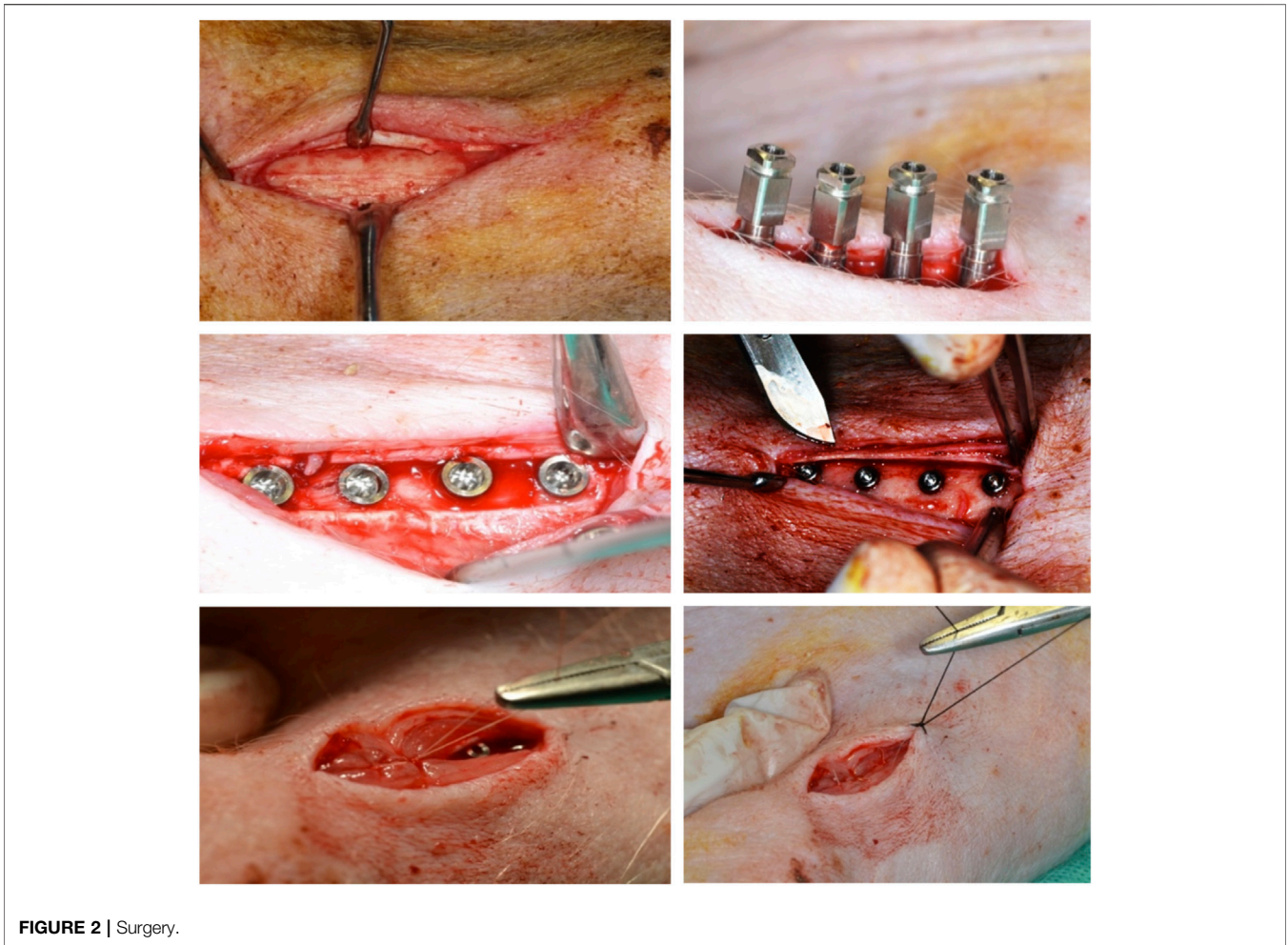
FIGURE 2 | Surgery.

antibiotic coverage to prevent surgical wound infection with amoxicillin (Clamoxyl®, Pfizer, New York, NY, United States) at a dose of 1.5 g, prepared as an injectable solution, intramuscularly for 5 days. The opioid analgesic used was intramuscular buprenorphine at a rate of 0.01–0.04 mg/kg, every 6–8 h (Buprex®, Quintiles, Danbury, CT, United States).

Preparation and Analysis of the Samples

Four weeks after implant placement, all the animals were sacrificed. The tibiae were extracted and kept in 10% formalin for at least 15 days before study. Subsequently, they were further processed following the protocol proposed by Donath and Breuer (Donath and Breuner, 1982). All samples and specimens were radiographed using a Schick Tecnologies® (Long Island City, NY 11101, United States) digital X-ray device. The cut and dehydrated specimens were embedded in methacrylate (Technovit 7,200®, VLC-Heraus Kulzer GMBH, Werheim, Germany). All samples with polished and treated surface were subjected to a staining process with the method of Lévai Laczkó (Jenö and Géza, 1975) for subsequent microscopic analysis.

An optical microscope (BX51, Olympus Corporation, Japan) connected to a camera and digital image analysis equipment (DP71, Cell-Sens Dimension 1.5, Olympus Corporation, Japan) was used for histomorphometric analysis of the samples. The stained samples were photographed with the digital camera at 40x magnification. The digitized images were processed at high resolution with the Cell Sens Dimensions computer system, Olympus, Japan. The digitized images were processed using software (Adobe Photoshop CS3, San Jose, CA, United States) and a digitizer tablet (Intuos 4 large, Wacom, Saitama, Japan).

The analysis of the measurements was performed according to the studies of Nkenke et al. and Kuchler et al. (Nkenke et al., 2005; Kuchler et al., 2013) with the following measurement protocol:

- Bone-to-implant contact (BIC).
- Bone-implant cortical contact (BICc).
- Percentage of new bone (BV/TV).
- Peri-implant bone density (Peri-implant Bone Area, Tissue Area, PBA/TA) and interthread bone density (Interthread Bone Area, Tissue Area, IBA/TA).

To generate homogeneous measurements, a 5 × 5 mm square around the coronal portion of the implants was assumed as the working area. The BIC was defined as the amount of implant perimeter surface in direct contact with the bone tissue; the bone density inside the threads (IBA/TA) was defined as the area of bone grown inside the threads, in relation to the total interthread space
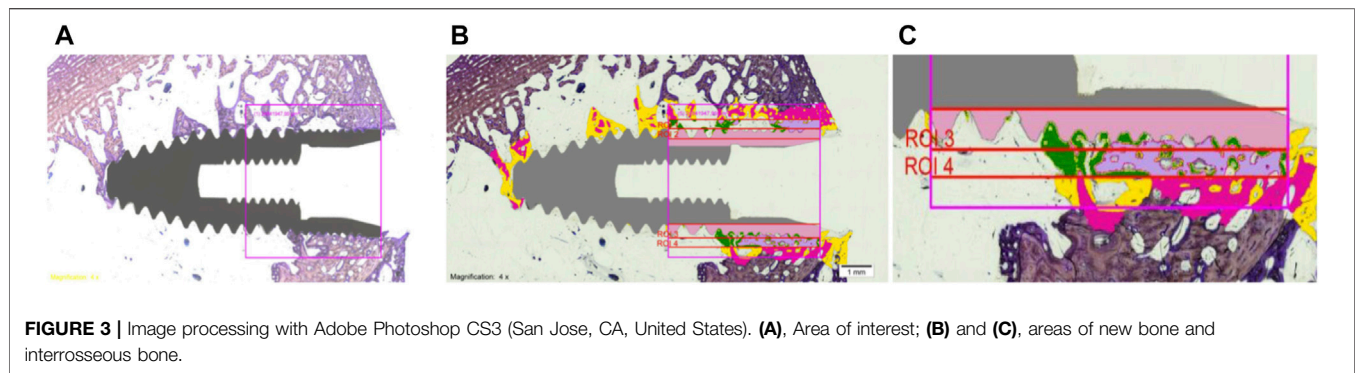
FIGURE 3 | Image processing with Adobe Photoshop CS3 (San Jose, CA, United States). **(A)**, Area of interest; **(B)** and **(C)**, areas of new bone and interrosseous bone.

TABLE 1 | Mean, standard deviation and p value in the groups for the different parameters.

Group	BIC	BICc	BV/TV	IBA/TA	PBA/TA
G1	19 ± 47.81	24.81 ± 55.37	13.28 ± 39.47	14.52 ± 34.39	32.98 ± 58.57
G2	34 ± 36.97	41.10 ± 63.86	16.38 ± 40.22	22.52 ± 45.28	29.36 ± 57.30
p value G1 vs. G2	0.527	0.345	0.046[a]	0.012[a]	0.293

BIC, bone implant contact; BICc, Bone-implant cortical contact; BV/TV, percentage of new bone; IBA/TA, interthread bone area; PBA/TA, Peri-implant Bone Area, Tissue Area.
[a]Statistical significance.

available; perimplant bone density (PBA/TA) was defined as the amount of bone generated in relation to the total implant surface at a distance of 0.3 mm from the implant and the percentage of new bone (BV/TV) was defined as the new bone present inside the threads, up to a distance of 0.3 mm away from the implant (**Figure 3**).

Statistical Analysis

The SPSS v.18 program was used. IBM (Chicago: SPSS Inc. United States). The statistical analysis was carried out in two distinct phases: the first using descriptive statistics to calculate the arithmetic mean, median, standard deviation, variance, range and standard error, expressing the values using a 95% confidence interval; the second, using inferential statistics with a significance level of $p <$ 0.05. Heterogeneity was calculated using the Kolmogorov-Smirnov test, Shapiro-Wilk test and Q-Q normality plots.

RESULTS

Statistical Results

Using a 95% confidence interval, with a significance level <0.05, statistical significance was found between G1 and G2 for BV/TV ($p = 0.04$) and IBA/TA ($p = 0.01$); for BIC, BICc and PBA/TA the differences between groups were not significant (**Table 1**).

Figures 4, 5 show boxplots and Q-Q (quantile-quantile) plots for BV-TV and IBA/TA for the experimental and control groups, respectively. The graph in **Figure 6** shows the difference in means between the experimental and control groups.

Histomorphometric Analysis

Histological analysis by light microscopy of longitudinal sections of the specimens revealed bone-to-implant contact with

interrupted medullary spaces at the bone-to-implant interface. No signs of fibrous tissue formation were found. **Figure 7** shows a total of 32 frames (16 for each experimental animal, 8 for each tibia). The first image of each frame shows the longitudinal section of the specimen before being processed by the software for data extraction. The second image of each frame shows the implants in gray color, in order to distinguish, by means of the software, the areas of old bone (in pink color), the areas of new bone (in yellow color) and the areas of soft tissue (in white color) (**Figure 7**). The highest values for BIC and BICc were obtained in the implants placed closer to the abdomen, in the right and left tibiae of G2 (46.47 and 63.83% respectively). The highest values for BV/TV and IBA/TA were obtained in the implants placed closer to the abdomen in the left tibiae of G1 (45.28 and 52.11% respectively).

DISCUSSION

The objective of our research was to determine the effect on osseointegration and early bone tissue formation of CEPA-treated and OPN-functionalized Ti implant surfaces compared to conventional etched surface implants in a minipig model.

The use of phosphonic acids for the purpose of bonding specific molecules, or simply to modify the microscopic properties of the implant surface, has been extensively studied. Esposito et al. (Esposito et al., 2013) evaluated, by means of a randomized clinical study, the clinical efficacy of a surface treatment of Ti dental implants using a monolayer of permanently bonded multiphosphonic acid molecules, mimicking the surface of natural hydroxyapatite, obtaining no

FIGURE 4 | Boxplot and Q-Q plot for BV-TV.

FIGURE 5 | Boxplot and Q-Q plot for IBA/TA.
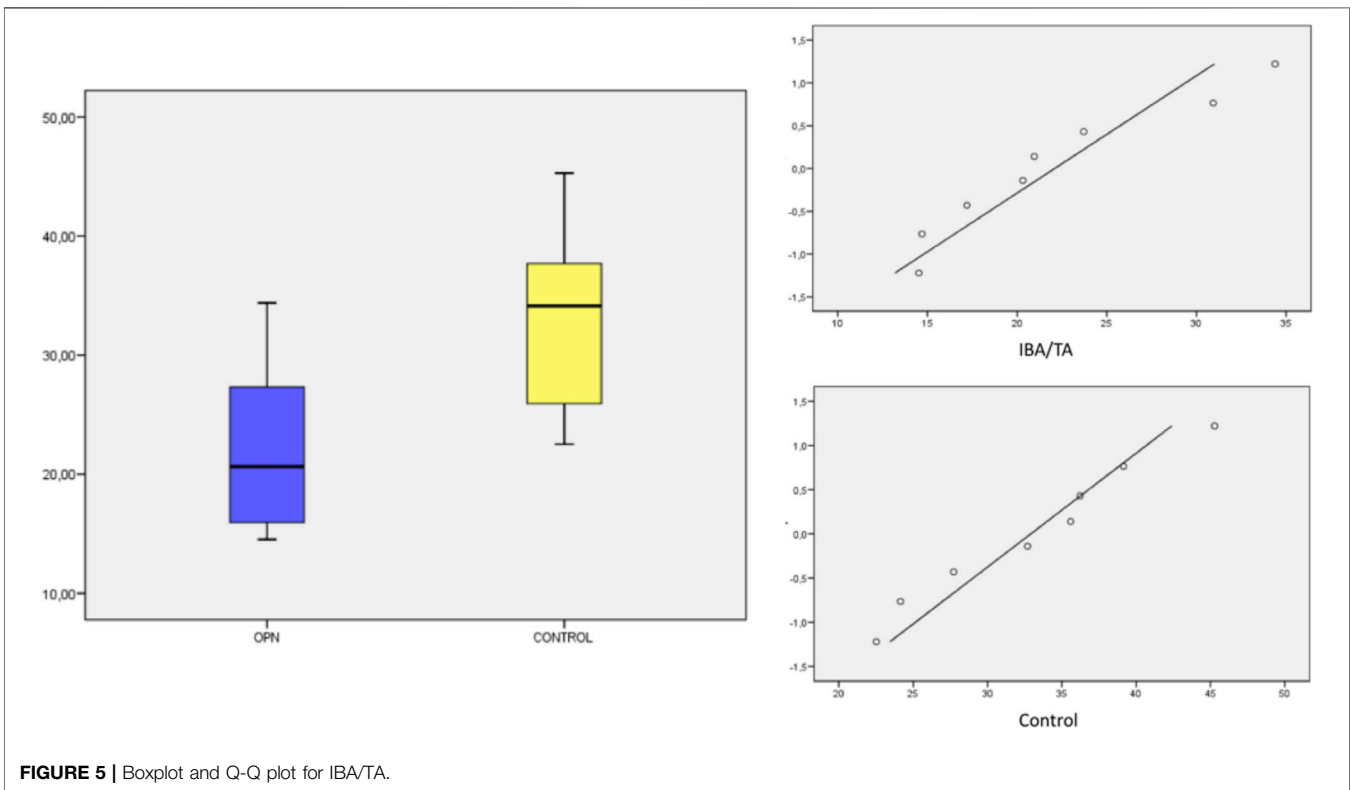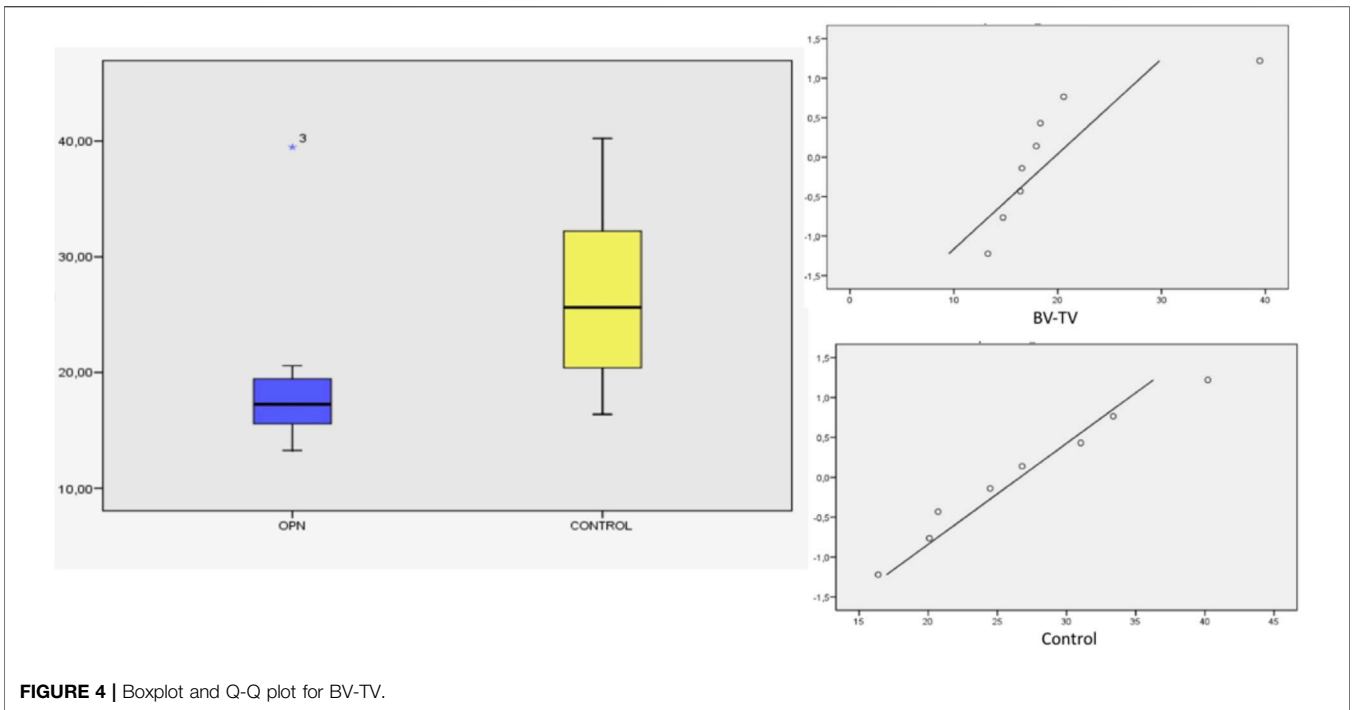
significant differences in terms of clinical healing with respect to the SLA surface control group. Maho et al. (Maho et al., 2013) studied the primary bone bioactivity of phosphonic acid

functionalized Ti substrates. Viornery et al. (Viornery et al., 2002) assessed the proliferation, differentiation and protein production of rat osteoblastic cells on phosphonic acid-

**FIGURE 6 |** Difference in means between experimental and control groups.
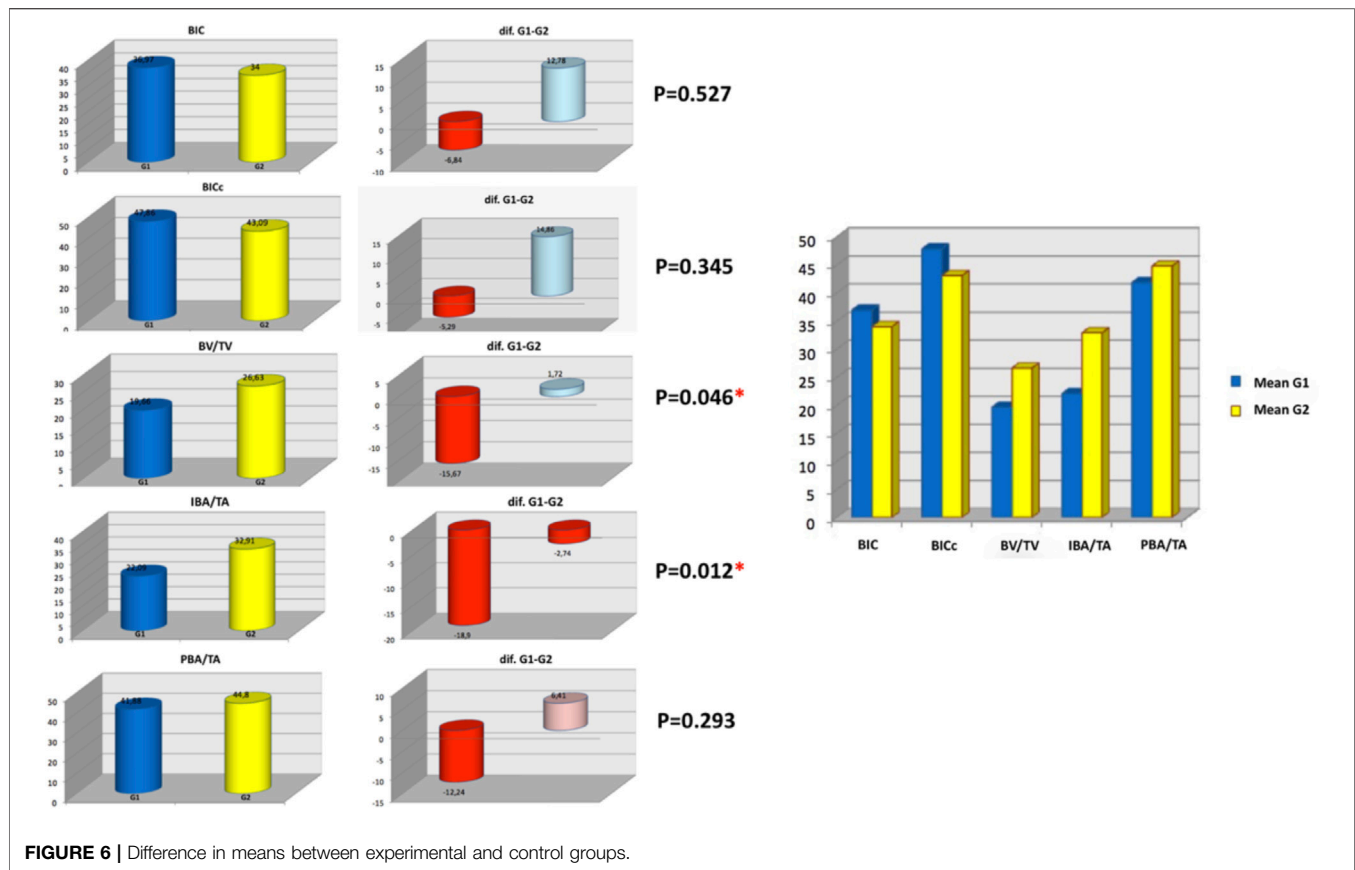
modified titanium surfaces *in vitro*, finding no statistical difference in osteoblast proliferation between phosphonic acid-modified titanium and unmodified titanium, which would indicate the absence of toxicity of phosphonic acids for the osteoblasts used in the study, however, they found that the synthesis of type I collagen was sensitive to surface modification and the total amount of protein synthesized was significantly higher than on unmodified titanium surfaces.

The ideal surface of dental implants should be one that is capable of inducing osseointegration, regardless of the implantation site and the quantity and quality of available bone (Fiorellini et al., 2016). Nowadays, research on distant osteogenesis has become a discovery of great importance, for the development of dental implant surfaces and therefore, different molecules have been proposed for the biochemical modification of surfaces, such as peptides, extracellular matrix proteins, growth factors and pharmacological agents (Meng et al., 2016; Tan and Al-Rubeai, 2019). Germanier et al. (Germanier et al., 2006) investigated on a minipig model, peptide-modified implant surfaces, finding a significant increase in BIC at 2 weeks compared to controls. Other studies have demonstrated the positive effect on peri-implant bone formation and osseointegration of Ti surfaces biochemically modified with collagen (Morra et al., 2006; Schliephake et al., 2006).

It should be noted that during the proliferative phase of osseointegration, fibroblasts are stimulated by growth factors to secrete extracellular matrix proteins such as collagen, chondroitin, fibronectin, vitronectin and other proteoglycans. The extracellular matrix provides a guide for osteoprogenitor cells, which migrate to the implant surface through integrin interaction (Terheyden et al., 2012). It has been proposed that osteoblasts originate from a subset of mesenchymal stem cells that line the minor vessels, called pericytes, and that after the release of bone morphogenetic protein (BMP), these cells differentiate into osteoblasts (Murray et al., 2014). Stadlinger et al. (Stadlinger et al., 2008) studied the osseointegration in pigs of implants coated with extracellular matrix components, suggesting that implants coated with chondroitinsulfate could lead to a higher degree of bone formation compared to control implants.

OPN has been shown to play a role in bone mineralization, wound healing, angiogenesis, cell adhesion, cell differentiation and foreign body response (Ishijima et al., 2007; Carvalho et al., 2018). Certain studies have found that some adhesion molecules, such as hyaluronic acid, fibronectin and OPN, together with OPN-derived synthetic adhesion peptides, are able to enhance the osseointegration of titanium surfaces *in vitro* (Lasa et al., 1997). Other *in vitro* investigations have studied different synthetic materials coated with OPN, with the purpose of exploring whether it could influence the functionality of biomaterial surfaces (Lee et al., 2003; Gordjestani et al., 2006; Liu et al., 2007; Bernards et al., 2008). Jensen et al. demonstrated *in vitro* that the bone mass density around OPN-coated hydroxyapatite surfaces were superior to uncoated surfaces, which would mean a great potential for OPN-coated biomaterials such as functional protein coatings, drug delivery systems in orthopedic implants, or scaffolds for tissue engineering (Jensen et al., 2010).
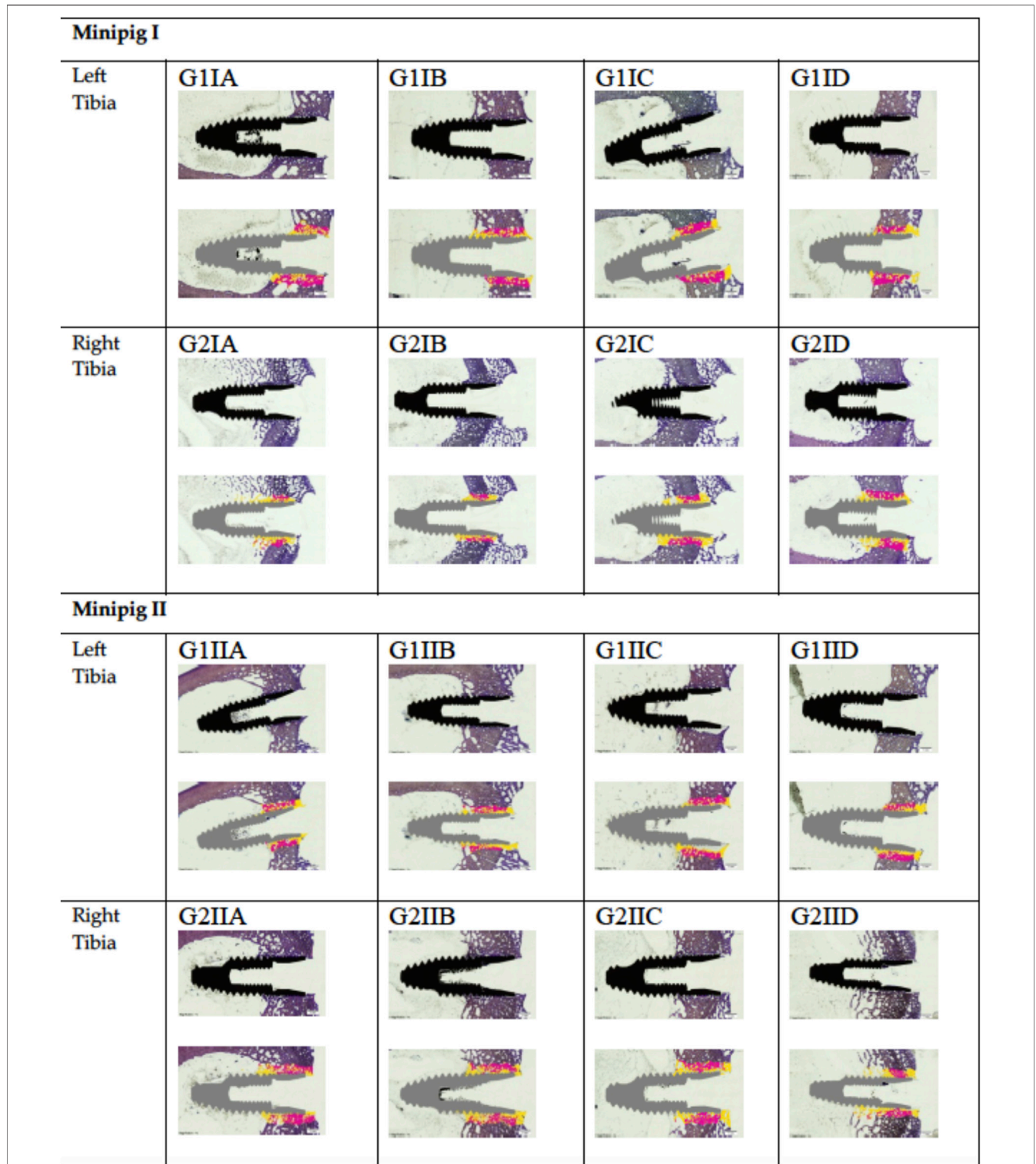
FIGURE 7 | Images of histomorphometric sections of all implants in the study in groups G1 and G2. **(A)** and **(B)** represent the osteotomies with the least and most proximity to the abdomen, respectively, and **(C)** and **(D)** the osteotomies with the least and most proximity to the hoof, respectively. The first image shows the longitudinal section of the specimen, before computer processing; the second image shows the photoshop-processed longitudinal section with the implants in gray and the areas of old bone (pink), areas of new bone (yellow) and areas of soft tissue (white).

OPN is naturally present on the non-organic surfaces of mineralized tissues, and several *in vivo* studies have examined the influence of OPN on the formation and remodeling of mineralized tissue (McKee and Nanci, 1996). Changes in mineralized tissue hardness, bone remodeling rate and vascularization have also been reported. In a rabbit cranial bone substitute model, OTP-coated coral HA granules were used (McKee and Nanci, 1996; McKee et al., 2011), and a positive effect of OPN on bone growth was observed; in addition, an inhibitory effect on the adverse foreign body reaction to implants has also been reported (Tsai et al., 2005; Liu et al., 2008). Asou et al. (Asou et al., 2001) used ectopically implanted bone discs in muscle in wild-type mice and compared them with OTP knockout mice; histological analysis indicated that the number of osteoclasts associated with the implanted discs was reduced in OPN knockout mice. In addition, they examined vascularization immunohistologically, and found that the number of vessels containing endothelial cells around the bone discs implanted in the muscle was reduced in the OTP knockout mice. This would indicate the link between OPN-dependent vascularization and osteoclast accumulation and that OPN is necessary for efficient vascularization by hemangiogenic endothelial cells and subsequent osteoclastic bone resorption.

Some *in vivo* studies have shown that differences in apoptosis rates would not explain the effects of OPN on vascularization, highlighting the possibility that vitronectin or other molecules may compensate for the absence of OPN in preventing apoptosis (McHugh et al., 2000; Lee et al., 2019).

The functional and structural characteristics of OPN predict a capacity of this protein to regulate calcification in the matrix of mineralized tissues and to participate, more specifically, in cell-matrix and matrix-matrix/mineral adhesion; it has been shown that OPN production is one of the first and last secretory activities of the osteoblast lineage and that this activity manifests, morphologically, as a limiting line at the interface of mineralized tissues at the bone matrix interface, implicating this protein in osteoclast adhesion and possibly in haptotaxis; it has even been suggested that it could act as a promoter of interfacial adhesion between opposing substrates, maintaining overall bone integrity during the bone remodeling sequence and resulting in an adherent between different dissimilar tissues or biocompatible materials such as osseointegrated implants (Wai and Kuo, 2004; Carvalho et al., 2021). Certain studies have reported that several types of bone tissue-related cells, such as osteoblasts and osteoclasts, are forced to mediate by OPN induction (Chellaiah and Hruska, 2003; Shin et al., 2004). However, some studies have recognized that OPN may have negative effects on the mineralization process, probably through inhibition of nucleation and growth of hydroxyapatite crystals (Pampena et al., 2004; Azzopardi et al., 2010).

Our study did not find statistical significance for BIC, BICc and PBA/TA values, in the OPN-functionalized implants, versus the control group, however, statistically significant values were found for BV/TV ($p = 0.04$) and IBA/TA ($p = 0.01$), results consistent with other recent studies, such as Makishi et al. who in a study in knockout mice, suggested that OPN-coated implants would enhance direct osteogenesis during osseointegration (Makishi et al., 2022). Implant healing time shows a large variation in the time of evaluation, ranging from 1 week to 6 months. Some studies

evaluate a single reading, while others have evaluated up to four readings. Our research established 4 weeks of waiting until euthanasia of the animals, although the tendency to healing over time was not analyzed, something that we consider to be one of the limitations of the study and that, if it had been extended (12 weeks, for example), different BIC results would have been obtained (Ramazanzadeh et al., 2014). On the other hand, another factor that seems to influence peri-implant bone formation is the anatomic location of the implant, since the dynamics of bone formation differ among the different locations (Jenny et al., 2016). In the same way, implants with wider diameters are associated with less bone formation (Jimbo et al., 2014). All this could have contributed to the poor results obtained in the experimental group for some of the parameters studied.

Finally, all research suggests that chemically nanostructured Ti surfaces can enhance endogenous extracellular OPN deposition by osteogenic cells *in vitro* as a function of etching time, a finding that should be taken into account in strategies for biofunctionalization of implant surfaces with cell-binding molecules (Bueno et al., 2011).

CONCLUSION

Based on the results obtained, it could be verified that the biofunctionalization of the Ti surface can be a good option to condition the biological processes that take place in the bone remodeling around dental implants. However, OPN should be carefully studied in different concentrations and at different times of bone remodeling, in extensive *in vivo* studies that allow us to perceive its real influence on the formation of a greater quantity and quality of peri-implant bone.

DATA AVAILABILITY STATEMENT

The original contributions presented in the study are included in the article/supplementary material, further inquiries can be directed to the corresponding author.

ETHICS STATEMENT

The animal study was reviewed and approved by Ethical Committee for Animal Experimentation of the Hospital Universitario Puerta de Hierro Majadahonda, Madrid, Spain. CEEA: 017/2013.

AUTHOR CONTRIBUTIONS

Conceptualization, JA and NL-V; methodology, JA and NL-V; software, CR; validation, JMA and AL-V; investigation, JA and NL-V; data curation, BM; writing—original draft preparation, AL-V; writing—review and editing, JMA; supervision, JMA All authors have read and agreed to the published version of the manuscript.

REFERENCES

Aragoneses, J., Suárez, A., López-Valverde, N., Martínez-Martínez, F., and Aragoneses, J. M. (2021). Assessment of the Tissue Response to Modification of the Surface of Dental Implants with Carboxyethylphosphonic Acid and Basic Fibroblastic Growth Factor Immobilization (Fgf-2): An Experimental Study on Minipigs. *Biology* 10 (5), 358. doi:10.3390/biology10050358

Aresti, A., Aragoneses, J., López-Valverde, N., Suárez, A., and Aragoneses, J. M. (2021). Effectiveness of Biofunctionalization of Titanium Surfaces with Phosphonic Acid. *Biomedicines* 9 (11), 1663. doi:10.3390/biomedicines9111663

Asou, Y., Rittling, S. R., Yoshitake, H., Tsuji, K., Shinomiya, K., Nifuji, A., et al. (2001). Osteopontin Facilitates Angiogenesis, Accumulation of Osteoclasts, and Resorption in Ectopic Bone*. *Endocrinology* 142, 1325–1332. doi:10.1210/endo.142.3.8006

Azzopardi, P. V., O'Young, J., Lajoie, G., Karttunen, M., Goldberg, H. A., and Hunter, G. K. (2010). Roles of Electrostatics and Conformation in Protein-Crystal Interactions. *PLoS ONE* 5, e9330. doi:10.1371/journal.pone.0009330

Bernards, M. T., Qin, C., and Jiang, S. (2008). MC3T3-E1 Cell Adhesion to Hydroxyapatite with Adsorbed Bone Sialoprotein, Bone Osteopontin, and Bovine Serum Albumin. *Colloids Surfaces B Biointerfaces* 64, 236–247. doi:10.1016/j.colsurfb.2008.01.025

Bueno, R. d. B. e. L., Adachi, P., Castro-Raucci, L. M. S. d., Rosa, A. L., Nanci, A., and Oliveira, P. T. d. (2011). Oxidative Nanopatterning of Titanium Surfaces Promotes Production and Extracellular Accumulation of Osteopontin. *Braz. Dent. J.* 22, 179–184. doi:10.1590/s0103-64402011000300001

Carvalho, M. S., Poundarik, A. A., Cabral, J. M. S., da Silva, C. L., and Vashishth, D. (2018). Biomimetic Matrices for Rapidly Forming Mineralized Bone Tissue Based on Stem Cell-Mediated Osteogenesis. *Sci. Rep.* 8, 14388. doi:10.1038/s41598-018-32794-4

Carvalho, M. S., Cabral, J. M. S., da Silva, C. L., and Vashishth, D. (2021). Bone Matrix Non-collagenous Proteins in Tissue Engineering: Creating New Bone by Mimicking the Extracellular Matrix. *Polymers* 13, 1095. doi:10.3390/polym13071095

Chellaiah, M. A., and Hruska, K. A. (2003). The Integrin {alpha} V {beta} 3 and CD44 Regulate the Actions of Osteopontin on Osteoclast Motility. *Calcif. Tissue Int.* 72, 197–205. doi:10.1007/s00223-002-1025-6

Chrcanovic, B. R., Albrektsson, T., and Wennerberg, A. (2014). Reasons for Failures of Oral Implants. *J. Oral Rehabil.* 41, 443–476. doi:10.1111/joor.12157

Coelho, P. G., Jimbo, R., Tovar, N., and Bonfante, E. A. (2015). Osseointegration: Hierarchical Designing Encompassing the Macrometer, Micrometer, and Nanometer Length Scales. *Dent. Mater.* 31, 37–52. doi:10.1016/j.dental.2014.10.007

Corne, P., De March, P., Cleymand, F., and Geringer, J. (2019). Fretting-corrosion Behavior on Dental Implant Connection in Human Saliva. *J. Mech. Behav. Biomed. Mater.* 94, 86–92. doi:10.1016/j.jmbbm.2019.02.025

Donath, K., and Breuner, G. (1982). A Method for the Study of Undecalcified Bones and Teeth with Attached Soft Tissues*. The Sage-Schliff (Sawing and Grinding) Technique. *J. Oral Pathol. Med.* 11, 318–326. doi:10.1111/j.1600-0714.1982.tb00172.x

Dunne, C. F., Twomey, B., Kelly, C., Simpson, J. C., and Stanton, K. T. (2015). Hydroxyapatite and Fluorapatite Coatings on Dental Screws: Effects of Blast Coating Process and Biological Response. *J. Mater Sci. Mater Med.* 26, 5347. doi:10.1007/s10856-014-5347-5

Esposito, M., Dojcinovic, I., Germon, L., Lévy, N., Curno, R., Buchini, S., et al. (2013). Safety and Efficacy of a Biomimetic Monolayer of Permanently Bound Multi-Phosphonic Acid Molecules on Dental Implants: 1 Year Post-loading Results from a Pilot Quadruple-Blinded Randomised Controlled Trial. *Eur. J. Oral Implantol.* 6, 227–236. PMID: 24179977.

Fiorellini, J., Glindmann, S., Salcedo, J., Weber, H.-P., Park, C.-J., and Sarmiento, H. (2016). The Effect of Osteopontin and an Osteopontin-Derived Synthetic Peptide Coating on Osseointegration of Implants in a Canine Model. *Int. J. Periodontics Restor. Dent.* 36, e88–e94. doi:10.11607/prd.2830

Germanier, Y., Tosatti, S., Broggini, N., Textor, M., and Buser, D. (2006). Enhanced Bone Apposition Around Biofunctionalized Sandblasted and Acid-Etched Titanium Implant Surfaces. A Histomorphometric Study in Miniature Pigs. *Clin. Oral Implants Res.* 17, 251–257. doi:10.1111/j.1600-0501.2005.01222.x

Gordjestani, M., Dermaut, L., De Ridder, L., De Waele, P., De Leersnijder, W., and Bosman, F. (2006). Osteopontin and Bone Metabolism in Healing Cranial Defects in Rabbits. *Int. J. Oral Maxillofac. Surg.* 35, 1127–1132. doi:10.1016/j.ijom.2006.07.002

Icer, M. A., and Gezmen-Karadag, M. (2018). The Multiple Functions and Mechanisms of Osteopontin. *Clin. Biochem.* 59, 17–24. doi:10.1016/j.clinbiochem.2018.07.003

Ishijima, M., Tsuji, K., Rittling, S. R., Yamashita, T., Kurosawa, H., Denhardt, D. T., et al. (2007). Osteopontin Is Required for Mechanical Stress-dependent Signals to Bone Marrow Cells. *J. Endocrinol.* 193, 235–243. doi:10.1677/joe.1.06704

Jenny, G., Jauernik, J., Bierbaum, S., Bigler, M., Grätz, K. W., Rücker, M., et al. (2016). A Systematic Review and Meta-Analysis on the Influence of Biological Implant Surface Coatings on Periimplant Bone Formation. *J. Biomed. Mat. Res.* 104, 2898–2910. doi:10.1002/jbm.a.35805

Jenö, L., and Géza, L. (1975). A Simple Differential Staining Method for Semi-thin Sections of Ossifying Cartilage and Bone Tissues Embedded in Epoxy Resin. *Mikroskopie* 31, 1–4. PMID: 51484.

Jensen, T., Dolatshahi-Pirouz, A., Foss, M., Baas, J., Lovmand, J., Duch, M., et al. (2010). Interaction of Human Mesenchymal Stem Cells with Osteopontin Coated Hydroxyapatite Surfaces. *Colloids Surfaces B Biointerfaces* 75, 186–193. doi:10.1016/j.colsurfb.2009.08.029

Jimbo, R., Janal, M. N., Marin, C., Giro, G., Tovar, N., and Coelho, P. G. (2014). The Effect of Implant Diameter on Osseointegration Utilizing Simplified Drilling Protocols. *Clin. Oral Impl. Res.* 25, 1295–1300. Epub 2013 Oct 8. doi:10.1111/clr.12268

Junker, R., Dimakis, A., Thoneick, M., and Jansen, J. A. (2009). Effects of Implant Surface Coatings and Composition on Bone Integration: a Systematic Review. *Clin. Oral Implants Res.* 20, 185–206. doi:10.1111/j.1600-0501.2009.01777.x

Klekotka, M., Dąbrowski, J. R., and Rećko, K. (2020). Fretting and Fretting Corrosion Processes of Ti6Al4V Implant Alloy in Simulated Oral Cavity Environment. *Materials* 13 (7), 1561. doi:10.3390/ma13071561

Kuchler, U., Pfingstner, G., Busenlechner, D., Dobsak, T., Reich, K., Heimel, P., et al. (2013). Osteocyte Lacunar Density and Area in Newly Formed Bone of the Augmented Sinus. *Clin. Oral Impl. Res.* 24, 285–289. doi:10.1111/j.1600-0501.2012.02533.x

Lasa, M., Chang, P.-L., Prince, C. W., and Pinna, L. A. (1997). Phosphorylation of Osteopontin by Golgi Apparatus Casein Kinase. *Biochem. Biophysical Res. Commun.* 240, 602–605. doi:10.1006/bbrc.1997.7702

Le Guéhennec, L., Soueidan, A., Layrolle, P., and Amouriq, Y. (2007). Surface Treatments of Titanium Dental Implants for Rapid Osseointegration. *Dent. Mater.* 23, 844–854. doi:10.1016/j.dental.2006.06.025

Lee, Y.-J., Park, S.-J., Lee, W.-K., Ko, J. S., and Kim, H.-M. (2003). MG63 Osteoblastic Cell Adhesion to the Hydrophobic Surface Precoated with Recombinant Osteopontin Fragments. *Biomaterials* 24, 1059–1066. doi:10.1016/s0142-9612(02)00439-8

Lee, G. S., Salazar, H. F., Joseph, G., Lok, Z. S. Y., Caroti, C. M., Weiss, D., et al. (2019). Osteopontin Isoforms Differentially Promote Arteriogenesis in Response to Ischemia via Macrophage Accumulation and Survival. *Lab. Invest.* 99, 331–345. doi:10.1038/s41374-018-0094-8

Liu, L., Qin, C., Butler, W. T., Ratner, B. D., and Jiang, S. (2007). Controlling the Orientation of Bone Osteopontin via its Specific Binding with Collagen I to Modulate Osteoblast Adhesion. *J. Biomed. Mat. Res.* 80A, 102–110. doi:10.1002/jbm.a.30858

Liu, L., Chen, G., Chao, T., Ratner, B. D., Sage, E. H., and Jiang, S. (2008). Reduced Foreign Body Reaction to Implanted Biomaterials by Surface Treatment with Oriented Osteopontin. *J. Biomaterials Sci. Polym. Ed.* 19, 821–835. doi:10.1163/156856208784522083

Maho, A., Detriche, S., Delhalle, J., and Mekhalif, Z. (2013). Sol-gel Synthesis of Tantalum Oxide and Phosphonic Acid-Modified Carbon Nanotubes Composite Coatings on Titanium Surfaces. *Mater. Sci. Eng. C* 33, 2686–2697. doi:10.1016/j.msec.2013.02.025

Makishi, S., Yamazaki, T., and Ohshima, H. (2022). Osteopontin on the Dental Implant Surface Promotes Direct Osteogenesis in Osseointegration. *Int. J. Mol. Sci.* 23, 1039. doi:10.3390/ijms23031039

McHugh, K. P., Hodivala-Dilke, K., Zheng, M.-H., Namba, N., Lam, J., Novack, D., et al. (2000). Mice Lacking β3 Integrins Are Osteosclerotic Because of Dysfunctional Osteoclasts. *J. Clin. Invest.* 105, 433–440. doi:10.1172/JCI8905

McKee, M. D., and Nanci, A. (1996). Osteopontin at Mineralized Tissue Interfaces in Bone, Teeth, and Osseointegrated Implants: Ultrastructural Distribution and

Implications for Mineralized Tissue Formation, Turnover, and Repair. *Microsc. Res. Tech.* 33, 141–164. doi:10.1002/(sici)1097-0029(19960201)33:2<141::aid-jemt5>3.0.co;2-w

McKee, M. D., Pedraza, C. E., and Kaartinen, M. T. (2011). Osteopontin and Wound Healing in Bone. *Cells Tissues Organs* 194, 313–319. doi:10.1159/000324244

Mendonça, G., Mendonça, D. B. S., Aragão, F. J. L., and Cooper, L. F. (2008). Advancing Dental Implant Surface Technology - from Micron- to Nanotopography. *Biomaterials* 29, 3822–3835. doi:10.1016/j.biomaterials.2008.05.012

Meng, H.-W., Chien, E. Y., and Chien, H.-H. (2016). Dental Implant Bioactive Surface Modifications and Their Effects on Osseointegration: a Review. *Biomark. Res.* 4, 24. doi:10.1186/s40364-016-0078-z

Morra, M., Cassinelli, C., Cascardo, G., Mazzucco, L., Borzini, P., Fini, M., et al. (2006). Collagen I-Coated Titanium Surfaces: Mesenchymal Cell Adhesion Andin Vivo Evaluation in Trabecular Bone Implants. *J. Biomed. Mat. Res.* 78A, 449–458. doi:10.1002/jbm.a.30783

Murray, I. R., West, C. C., Hardy, W. R., James, A. W., Park, T. S., Nguyen, A., et al. (2014). Natural History of Mesenchymal Stem Cells, from Vessel Walls to Culture Vessels. *Cell. Mol. Life Sci.* 71, 1353–1374. doi:10.1007/s00018-013-1462-6

Nkenke, E., Fenner, M., Vairaktaris, E. G., Neukam, F. W., and Radespiel-Tröger, M. (2005). Immediate versus Delayed Loading of Dental Implants in the Maxillae of Minipigs. Part II: Histomorphometric Analysis. *Int. J. Oral Maxillofac. Implants* 20, 540–546. PMID: 16161738.

Ogle, O. E. (2015). Implant Surface Material, Design, and Osseointegration. *Dent. Clin. N. Am.* 59, 505–520. doi:10.1016/j.cden.2014.12.003

Pampena, D. A., Robertson, K. A., Litvinova, O., Lajoie, G., Goldberg, H. A., and Hunter, G. K. (2004). Inhibition of Hydroxyapatite Formation by Osteopontin Phosphopeptides. *Biochem. J.* 378, 1083–1087. doi:10.1042/BJ20031150

Pellegrini, G., Francetti, L., Barbaro, B., and Del Fabbro, M. (2018). Novel Surfaces and Osseointegration in Implant Dentistry. *J. Invest. Clin. Dent.* 9, e12349. doi:10.1111/jicd.12349

Ramazanzadeh, B. A., Fatemi, K., Dehghani, M., Mohtasham, N., Jahanbin, A., and Sadeghian, H. (2014). Effect of Healing Time on Bone-Implant Contact of Orthodontic Micro-implants: a Histologic Study. *ISRN Dent.* 2014, 1–7. doi:10.1155/2014/179037

Ren, B., Wan, Y., Liu, C., Wang, H., Yu, M., Zhang, X., et al. (2021). Improved Osseointegration of 3D Printed Ti-6Al-4V Implant with a Hierarchical Micro/nano Surface Topography: An *In Vitro* and *In Vivo* Study. *Mater. Sci. Eng. C* 118, 111505. doi:10.1016/j.msec.2020.111505

Schliephake, H., Scharnweber, D., Roesseler, S., Dard, M., Sewing, A., and Aref, A. (2006). Biomimetic Calcium Phosphate Composite Coating of Dental Implants. *Int. J. Oral Maxillofac. Implants* 21, 738–746. PMID: 17066635.

Shin, H., Zygourakis, K., Farach-Carson, M. C., Yaszemski, M. J., and Mikos, A. G. (2004). Attachment, Proliferation, and Migration of Marrow Stromal Osteoblasts Cultured on Biomimetic Hydrogels Modified with an Osteopontin-Derived Peptide. *Biomaterials* 25, 895–906. doi:10.1016/s0142-9612(03)00602-1

Smeets, R., Henningsen, A., Jung, O., Heiland, M., Hammächer, C., and Stein, J. M. (2014). Definition, Etiology, Prevention and Treatment of Peri-Implantitis - a Review. *Head. Face Med.* 10, 34. doi:10.1186/1746-160X-10-34

Smeets, R., Stadlinger, B., Schwarz, F., Beck-Broichsitter, B., Jung, O., Precht, C., et al. (2016). Impact of Dental Implant Surface Modifications on Osseointegration. *BioMed Res. Int.* 2016, 1–16. doi:10.1155/2016/6285620

Stadlinger, B., Pilling, E., Huhle, M., Mai, R., Bierbaum, S., Scharnweber, D., et al. (2008). Evaluation of Osseointegration of Dental Implants Coated with Collagen, Chondroitin Sulphate and BMP-4: an Animal Study. *Int. J. Oral Maxillofac. Surg.* 37, 54–59. doi:10.1016/j.ijom.2007.05.024

Tan, F., and Al-Rubeai, M. (2019). Customizable Implant-specific and Tissue-specific Extracellular Matrix Protein Coatings Fabricated Using Atmospheric Plasma. *Front. Bioeng. Biotechnol.* 7, 247. doi:10.3389/fbioe.2019.00247

Terheyden, H., Lang, N. P., Bierbaum, S., and Stadlinger, B. (2012). Osseointegration - Communication of Cells. *Clin. Oral Impl. Res.* 23, 1127–1135. doi:10.1111/j.1600-0501.2011.02327.x

Tsai, A. T., Rice, J., Scatena, M., Liaw, L., Ratner, B. D., and Giachelli, C. M. (2005). The Role of Osteopontin in Foreign Body Giant Cell Formation. *Biomaterials* 26, 5835–5843. doi:10.1016/j.biomaterials.2005.03.003

Türker, N. S., Özer, A. Y., Kutlu, B., Nohutcu, R., Sungur, A., Bilgili, H., et al. (2014). The Effect of Gamma Radiation Sterilization on Dental Biomaterials. *Tissue Eng. Regen. Med.* 11, 341–349. doi:10.1007/s13770-014-0016-9

Ueno, T., Takeuchi, M., Hori, N., Iwasa, F., Minamikawa, H., Igarashi, Y., et al. (2012). Gamma Ray Treatment Enhances Bioactivity and Osseointegration Capability of Titanium. *J. Biomed. Mat. Res.* 100B, 2279–2287. doi:10.1002/jbm.b.32799

Viornery, C., Guenther, H. L., Aronsson, B.-O., Péchy, P., Descouts, P., and Grätzel, M. (2002). Osteoblast Culture on Polished Titanium Disks Modified with Phosphonic Acids. *J. Biomed. Mat. Res.* 62, 149–155. doi:10.1002/jbm.10205

Wai, P. Y., and Kuo, P. C. (2004). The Role of Osteopontin in Tumor Metastasis. *J. Surg. Res.* 121, 228–241. doi:10.1016/j.jss.2004.03.028

Yuan, X., Pei, X., Zhao, Y., Li, Z., Chen, C. H., Tulu, U. S., et al. (2018). Biomechanics of Immediate Postextraction Implant Osseointegration. *J. Dent. Res.* 97, 987–994. doi:10.1177/0022034518765757

Zhang, J., Liu, J., Wang, C., Chen, F., Wang, X., and Lin, K. (2020). A Comparative Study of the Osteogenic Performance between the Hierarchical Micro/submicro-Textured 3D-Printed Ti6Al4V Surface and the SLA Surface. *Bioact. Mater.* 5, 9–16. doi:10.1016/j.bioactmat.2019.12.008

Zhao, G., Raines, A., Wieland, M., Schwartz, Z., and Boyan, B. (2007). Requirement for Both Micron- and Submicron Scale Structure for Synergistic Responses of Osteoblasts to Substrate Surface Energy and Topography. *Biomaterials* 28, 2821–2829. doi:10.1016/j.biomaterials.2007.02.024